Cosmological constraints from Subaru HSC Y3 weak lensing observations

Surhud More (IUCAA)
On behalf of the Subaru HSC collaboration

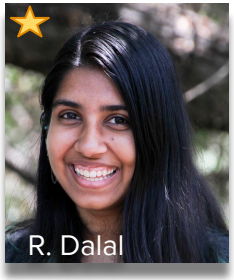
Nov 1, 2024 KIAS Workshop, Gyeongju

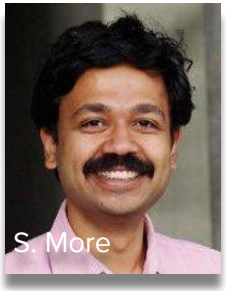
HSC Weak lensing working group



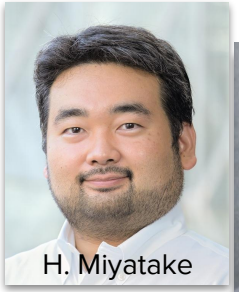










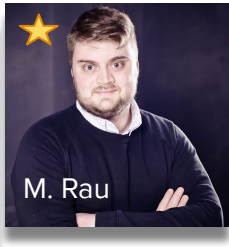






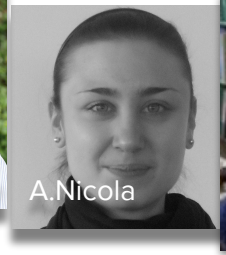












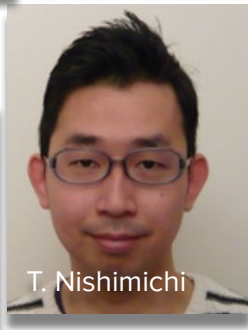












And efforts of many more!

Key weak lensing group publications: HSC Year 3

- The three-year shear catalog of the Subaru Hyper Suprime-Cam SSP Survey (**Li X.**, et al. 2022, PASJ, 74, 2)
- A General Framework for Removing Point Spread Function Additive Systematics in Cosmological Weak Lensing Analysis (**Zhang T.** et al. 2022, MNRAS submitted, arXiv:2212.03257)
- Weak Lensing Tomographic Redshift Distribution Inference for the Hyper Suprime-Cam Subaru Strategic Program three-year shape catalogue (**Rau, M.** et al. 2022, MNRAS, submitted, arXiv:2211.16516)
- Hyper Suprime-Cam Year 3 Results: Cosmology from Cosmic Shear Two-Point Correlation Functions (**Li X.,** et al. 2023, PRD, to be submitted)
- Hyper Suprime-Cam Year 3 Results: Cosmology from Cosmic Shear Power Spectra (**Dalal R.,** et al. 2023, PRD, to be submitted)
- Hyper Suprime-Cam Year 3 Results: Measurements of the Clustering of SDSS-BOSS galaxies, galaxy-galaxy lensing and cosmic shear (More S., et al. 2023, PRD, to be submitted)
- Hyper Suprime-Cam Year 3 Results: Cosmology from Galaxy Clustering and Weak Lensing with HSC and SDSS using the Minimal Bias Model (**Sugiyama S.,** et al. 2023, PRD, to be submitted)
- Hyper Suprime-Cam Year 3 Results: Cosmology from Galaxy Clustering and Weak Lensing with HSC and SDSS using the Emulator Based Halo Model (Miyatake H., et al. 2023, PRD, to be submitted)

https://hsc-release.mtk.nao.ac.jp/doc/index.php/wly3/

Early career scientists leading the projects marked in bold

Gravitational lensing: Witnessing growth of structure

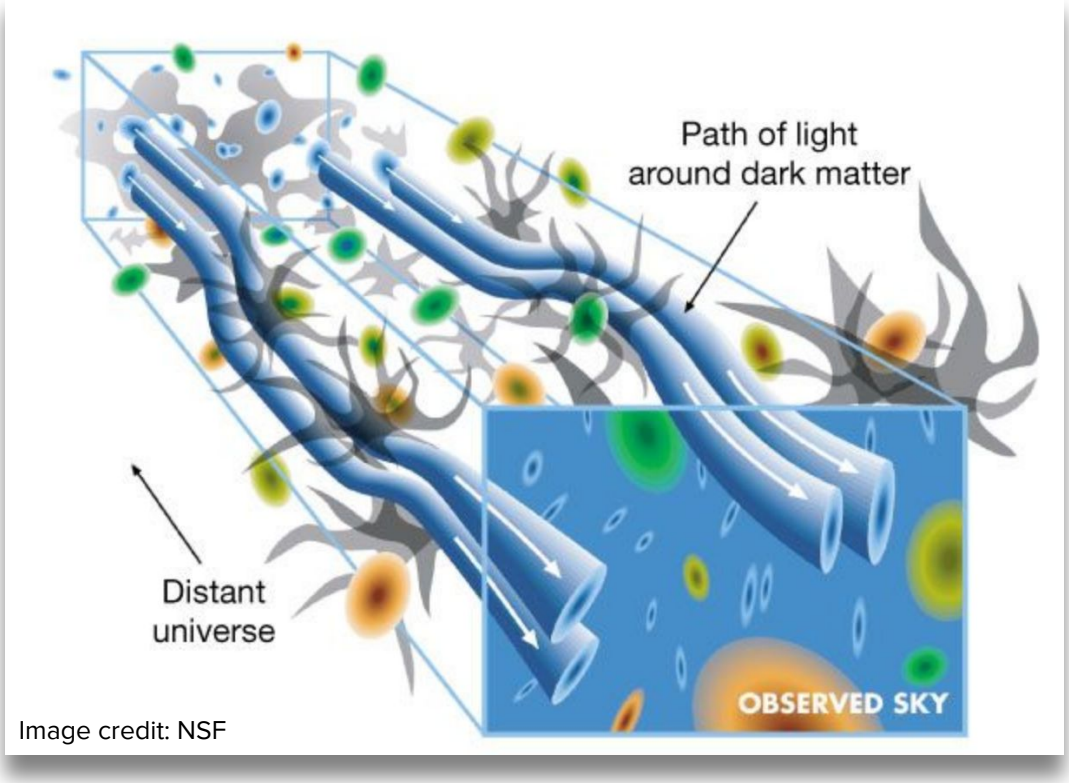
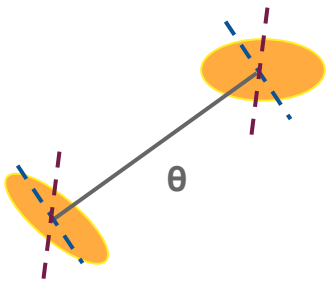


Image credit: NSF

- Weak gravitational lensing causes changes to the shape of the background galaxies
- Possible to carry out weak lensing tomography by selecting source galaxies at different distances away from us.

Cosmic shear correlations



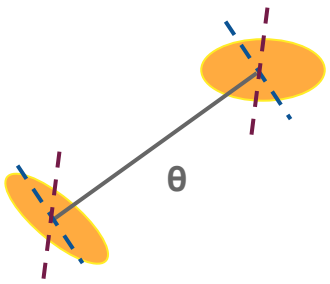
1. 2D Shapes have Magnitudes and Angles
2. Tangential correlation(ξ_+)
3. 45 degree correlation (ξ_-)

$$\xi_{\pm}(\theta) = \langle \gamma_t \gamma_t \rangle (\theta) \pm \langle \gamma_\times \gamma_\times \rangle (\theta) \,, \quad \xi_\times(\theta) = \langle \gamma_t \gamma_\times \rangle (\theta)$$

$$\xi_+(\theta) = \int_0^\infty \frac{\mathrm{d}\ell\,\ell}{2\pi} \mathrm{J}_0(\ell\theta)\, P_\kappa(\ell) \,; \quad \xi_-(\theta) = \int_0^\infty \frac{\mathrm{d}\ell\,\ell}{2\pi} \mathrm{J}_4(\ell\theta)\, P_\kappa(\ell) \,,$$

$$P_{12}^{\kappa}(\ell) = \int_0^{\chi_s} d\chi_d \frac{q_1(\chi_d) q_2(\chi_d)}{\chi_d^2} P_\delta\left(\frac{\ell}{\chi_d}, \chi_d\right)$$

Cosmic shear correlations



1. 2D Shapes have Magnitudes and Angles
2. Tangential correlation(ξ_+)
3. 45 degree correlation (ξ_-)

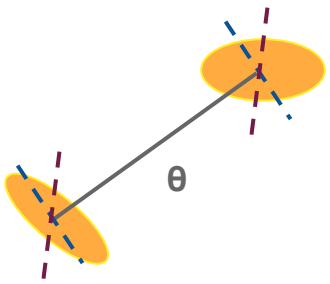
Well calibrated measurement of shapes

$$\xi_{\pm}(\theta) = \langle \gamma_t \gamma_t \rangle(\theta) \pm \langle \gamma_\times \gamma_\times \rangle(\theta), \quad \xi_\times(\theta) = \langle \gamma_t \gamma_\times \rangle(\theta)$$

$$\xi_+(\theta) = \int_0^\infty \frac{d\ell\,\ell}{2\pi} J_0(\ell\theta)\, P_\kappa(\ell)\,; \quad \xi_-(\theta) = \int_0^\infty \frac{d\ell\,\ell}{2\pi} J_4(\ell\theta)\, P_\kappa(\ell)\,,$$

$$P_{12}^{\kappa}(\ell) = \int_0^{\chi_s} d\chi_d \frac{q_1(\chi_d) q_2(\chi_d)}{\chi_d^2} P_\delta\left(\frac{\ell}{\chi_d}, \chi_d\right)$$

Cosmic shear correlations



1. 2D Shapes have Magnitudes and Angles
2. Tangential correlation(ξ_+)
3. 45 degree correlation (ξ_-)

Well calibrated measurement of shapes

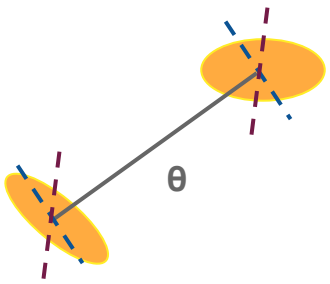
$$\xi_{\pm}(\theta) = \langle \gamma_t \gamma_t \rangle (\theta) \pm \langle \gamma_\times \gamma_\times \rangle (\theta), \quad \xi_\times(\theta) = \langle \gamma_t \gamma_\times \rangle (\theta)$$

$$\xi_+(\theta) = \int_0^\infty \frac{\mathrm{d}\ell\,\ell}{2\pi} \mathrm{J}_0(\ell\theta)\, P_\kappa(\ell)\,; \quad \xi_-(\theta) = \int_0^\infty \frac{\mathrm{d}\ell\,\ell}{2\pi} \mathrm{J}_4(\ell\theta)\, P_\kappa(\ell)\,,$$

Well understood redshifts of source galaxies

$$P_{12}^{\kappa}(\ell) = \int_0^{\chi_s} d\chi_d \frac{q_1(\chi_d) q_2(\chi_d)}{\chi_d^2} P_\delta\left(\frac{\ell}{\chi_d}, \chi_d\right)$$

Cosmic shear correlations



1. 2D Shapes have Magnitudes and Angles
2. Tangential correlation(ξ_+)
3. 45 degree correlation (ξ_-)

Well calibrated measurement of shapes

$$\xi_{\pm}(\theta) = \langle \gamma_t \gamma_t \rangle(\theta) \pm \langle \gamma_\times \gamma_\times \rangle(\theta), \quad \xi_\times(\theta) = \langle \gamma_t \gamma_\times \rangle(\theta)$$

$$\xi_+(\theta) = \int_0^\infty \frac{d\ell\,\ell}{2\pi} J_0(\ell\theta)\, P_\kappa(\ell)\,; \quad \xi_-(\theta) = \int_0^\infty \frac{d\ell\,\ell}{2\pi} J_4(\ell\theta)\, P_\kappa(\ell)\,,$$

Well understood redshifts of source galaxies

$$P_{12}^\kappa(\ell) = \int_0^{\chi_s} d\chi_d \frac{q_1(\chi_d) q_2(\chi_d)}{\chi_d^2} P_\delta\left(\frac{\ell}{\chi_d}, \chi_d\right)$$

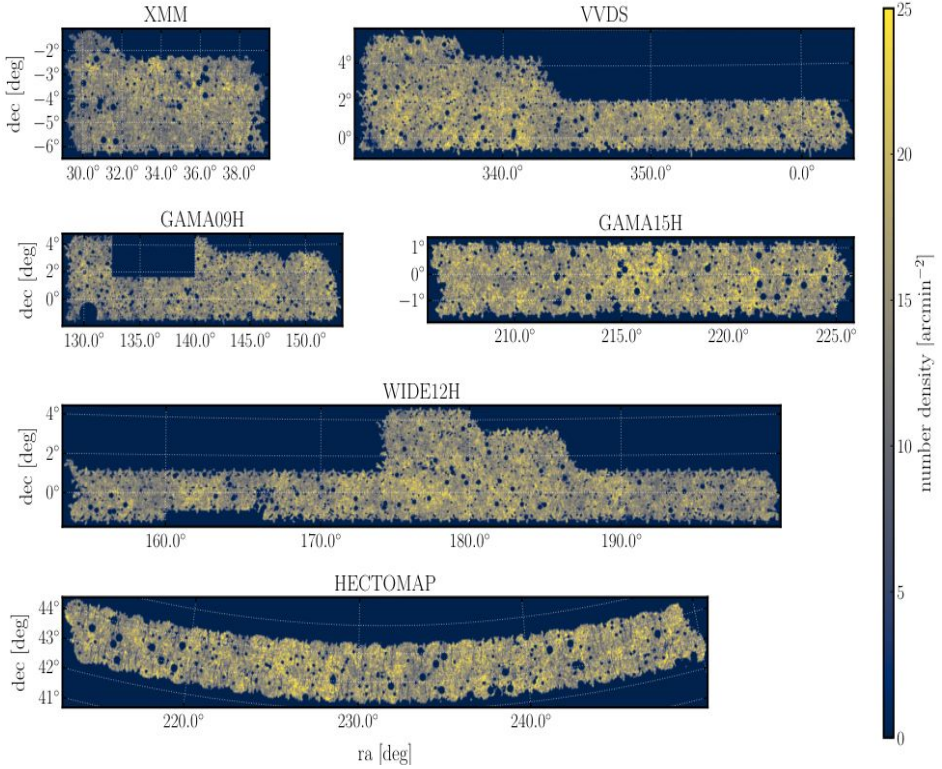
Good model for the matter power spectrum

Li, .. SM, et al. 2022

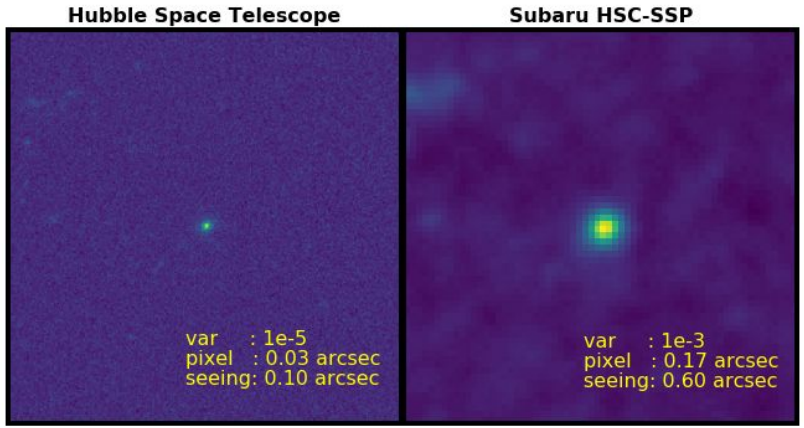
Subaru telescope: Hyper Suprime-Cam survey



- 1100 sq deg grizy imaging in excellent conditions.
- i-band median seeing of 0.6”



Shape measurement characterizations

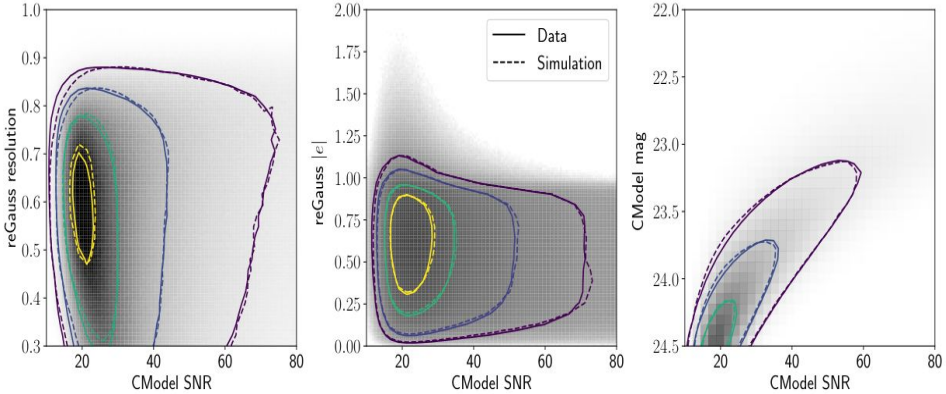


Mandelbaum+ (2018), Li+ (2022)

$$\hat{\gamma} = (1 + m)\gamma + c$$

Measured shape — input shape

Quantify **biases** with **image simulations**.



Li, .. SM, et al. 2022

1. We use galaxy image simulations (downgrading the high-resolution Hubble Space Telescope **(HST)** images to the HSC observational conditions) to calibrate our shape estimation;

2. Our simulation matches the galaxy number histogram with an accuracy of **1%.**

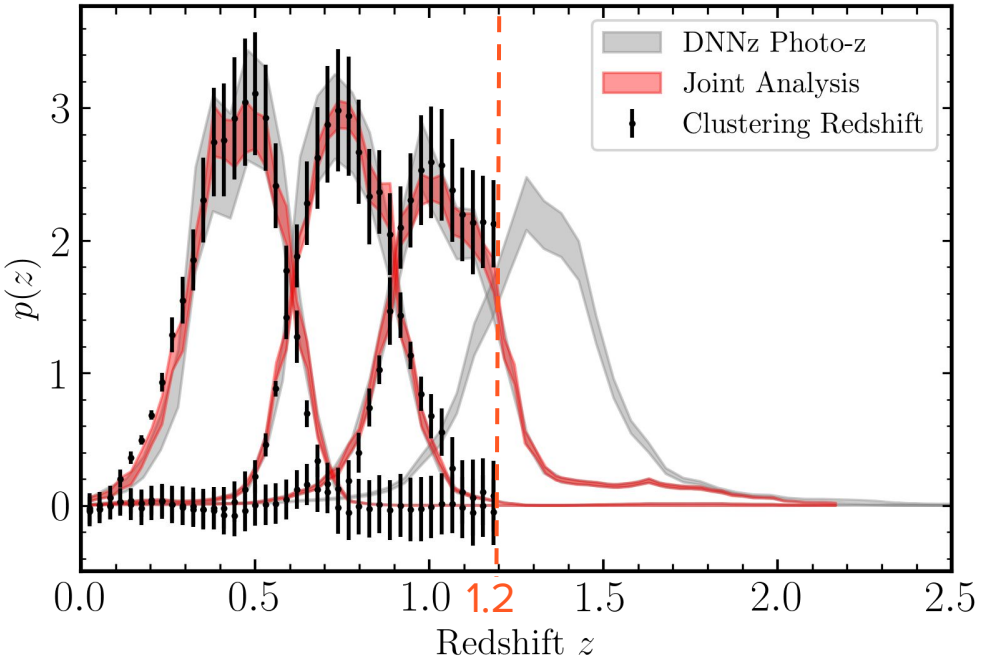
3. **The image simulation describes the i-band images well and therefore our ability to control and quantify systematic errors in the shape catalog.**

Redshift distribution inference

Grey: photo-z likelihood (DNNz) + cosmic variance

Clustering Redshift: cross-correlation between HSC source catalog and CAMIRA-LRG

Red: joint posterior of the two

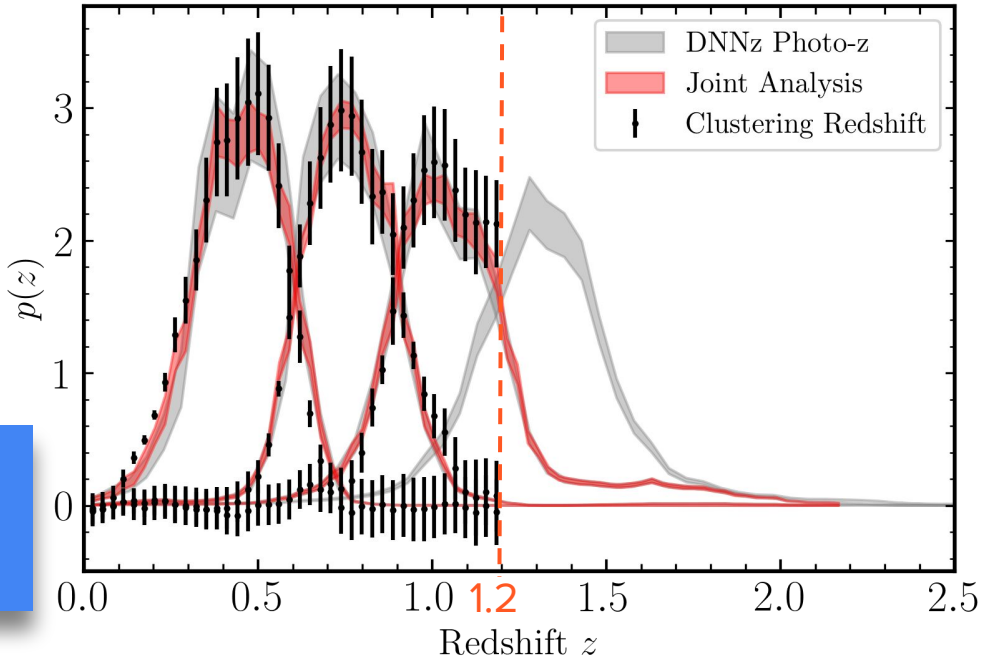


Redshift distribution inference

Grey: photo-z likelihood (DNNz) + cosmic variance

Clustering Redshift: cross-correlation between HSC source catalog and CAMIRA-LRG

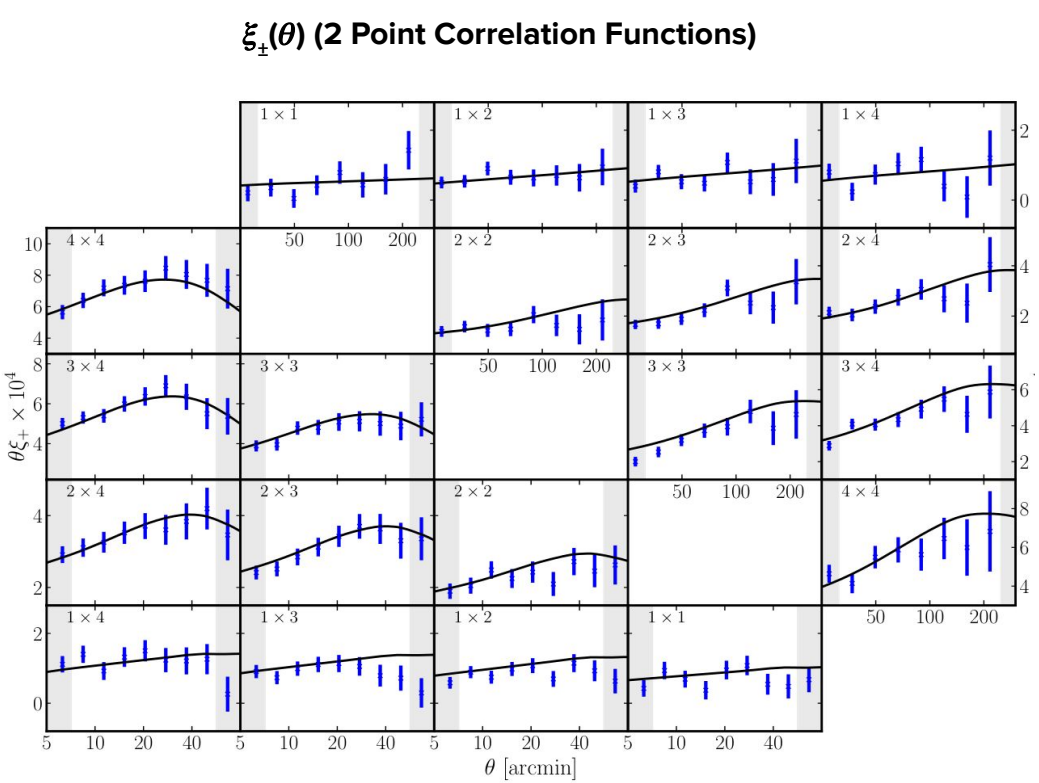
Red: joint posterior of the two



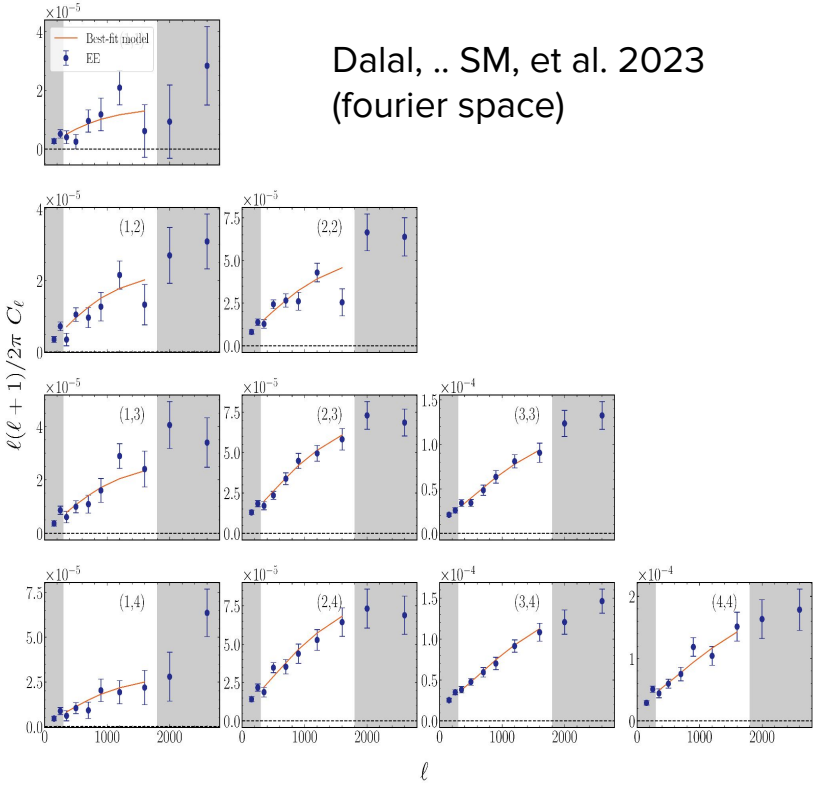
Informative priors: Trust photo-z analysis for all bins

Uninformative priors: Bin 3 and Bin 4 shifted by arbitrary Delta z

Cosmic shear measurements

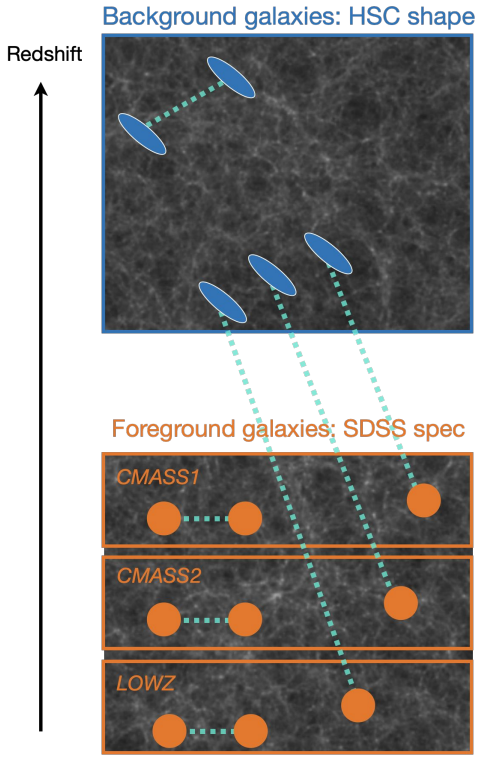


Li, .. SM, et al. 2023 (Real space)

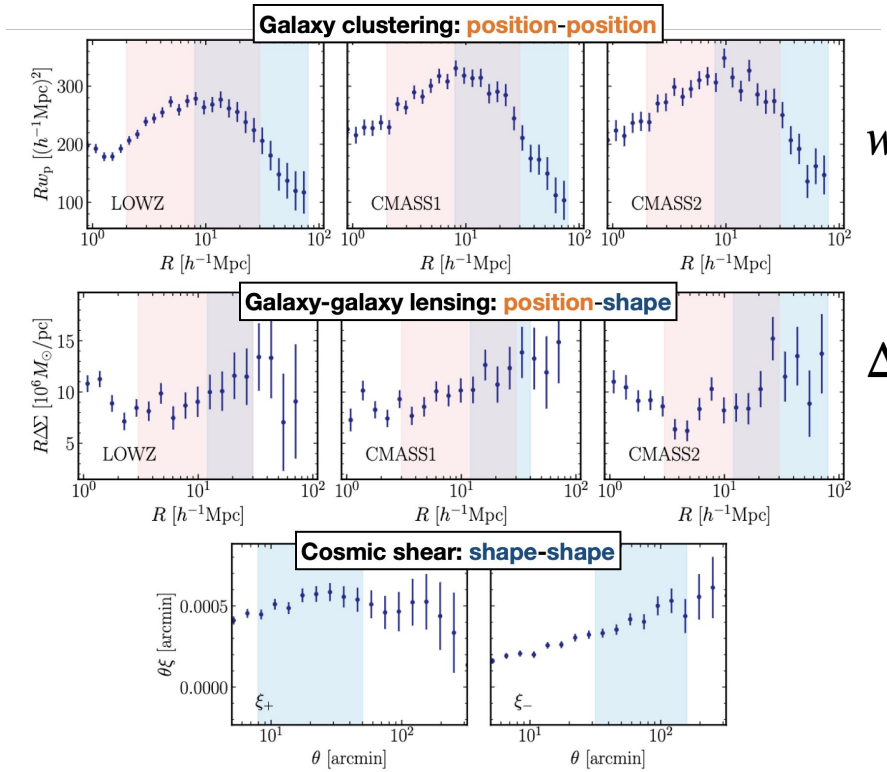


Dalal, .. SM, et al. 2023 (fourier space)

3x2pt analysis with HSC x SDSS catalogs



Credit: T. Nishimichi, edited by S. Sugiyama



$\delta_g = b\delta_m$ on large scales

$w_p \sim b^2 \xi_{mm}(r\,|\,\Omega_m, \sigma_8)$

$\Delta\Sigma \sim b\xi_{mm}(r\,|\,\Omega_m, \sigma_8)$

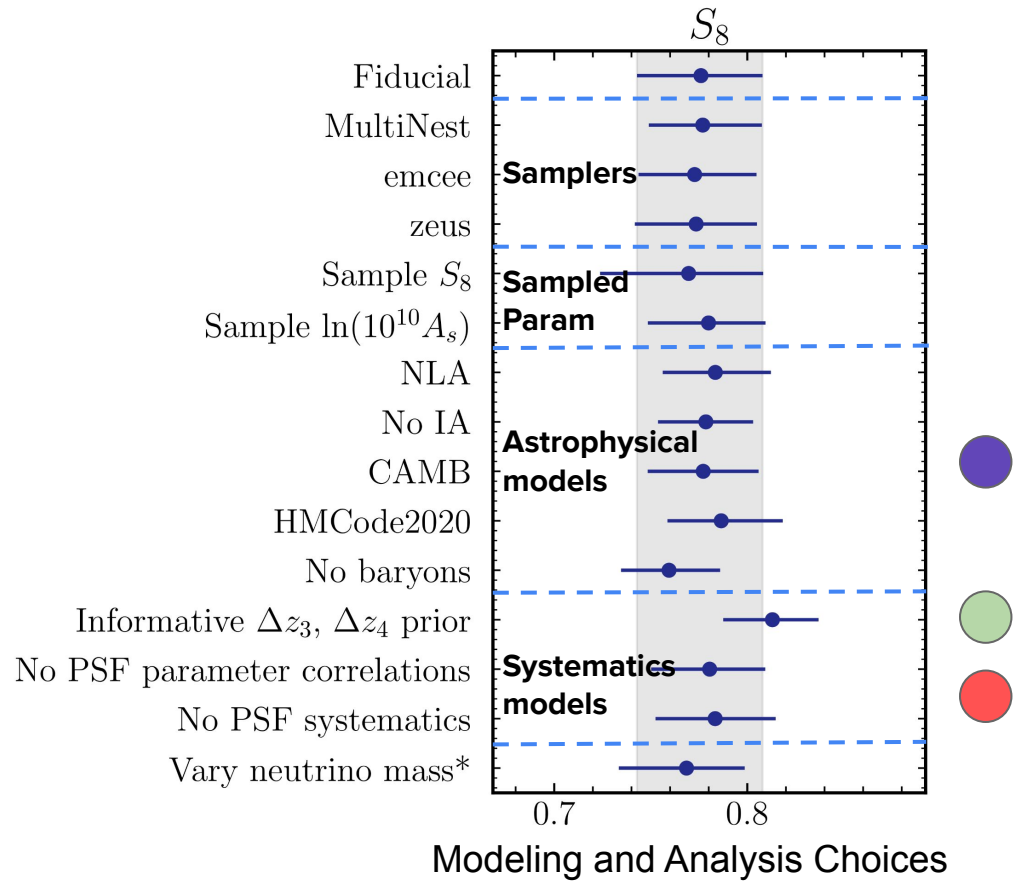
$\xi_\pm \sim \xi_{mm}(r\,|\,\Omega_m, \sigma_8)$

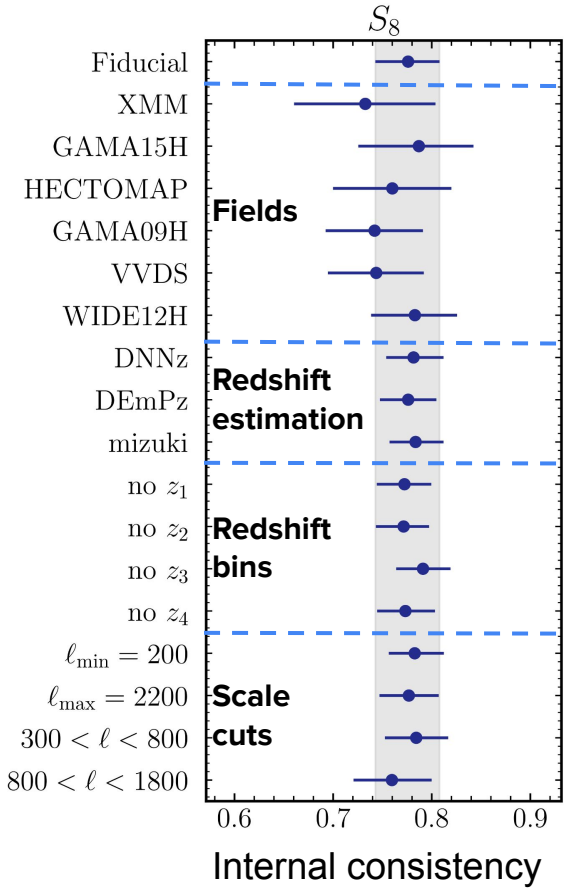
The data vector passed systematics tests in the scales shown by shaded region. These scales were used for the 3x2 pt cosmology analyses.

Cosmic shear analysis

$$S_8 = 0.776^{+0.032}_{-0.033}$$

Dalal, .. SM, et al. 2023
(fourier space)

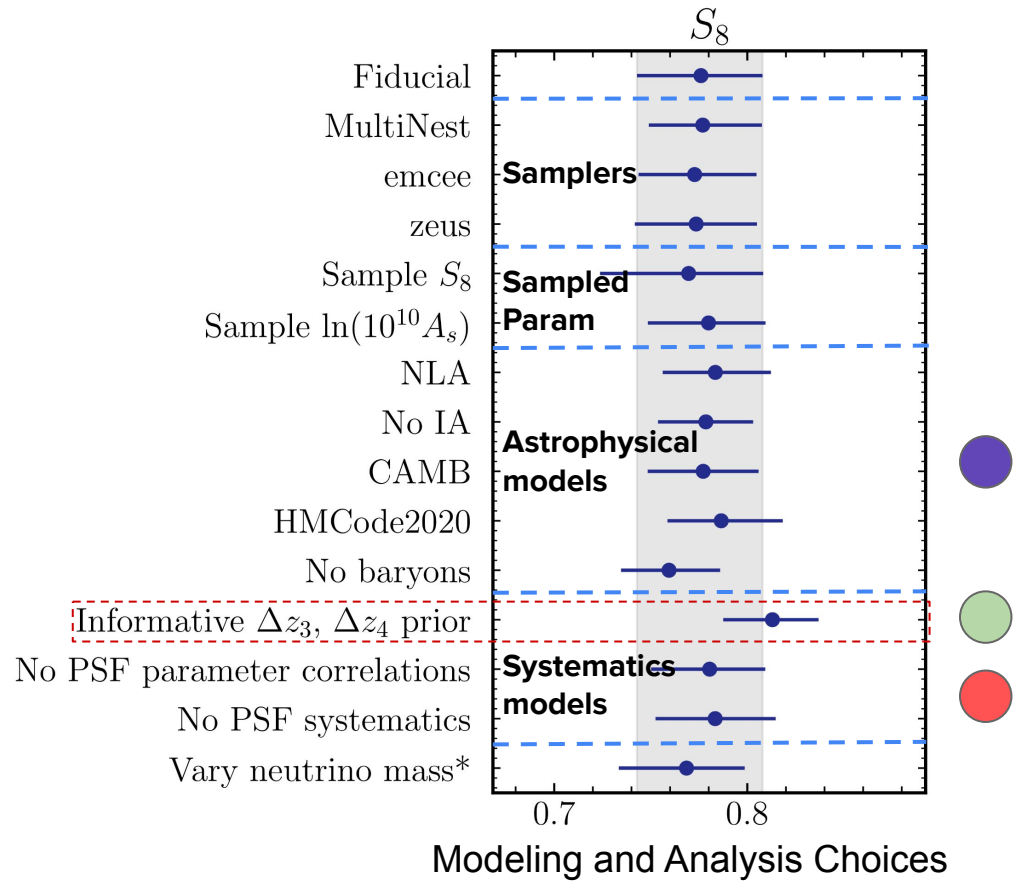


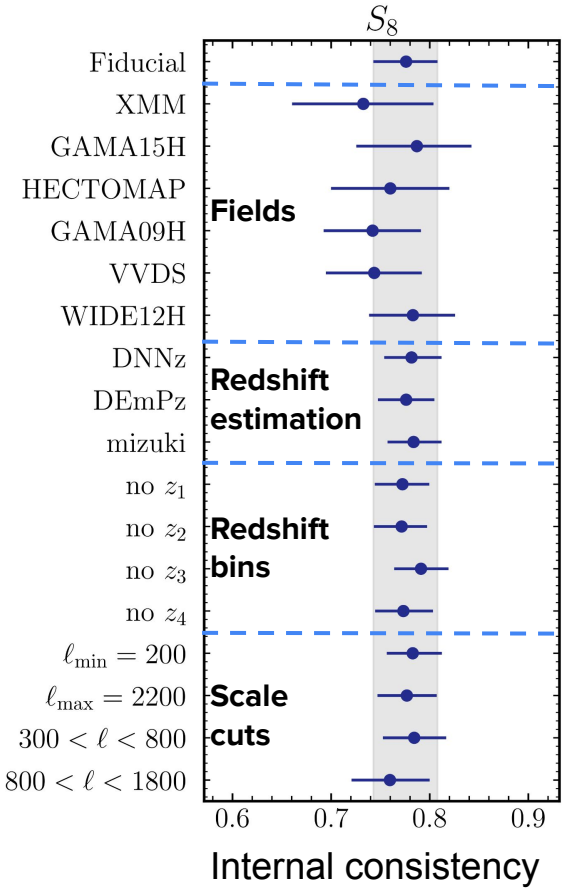


Cosmic shear analysis

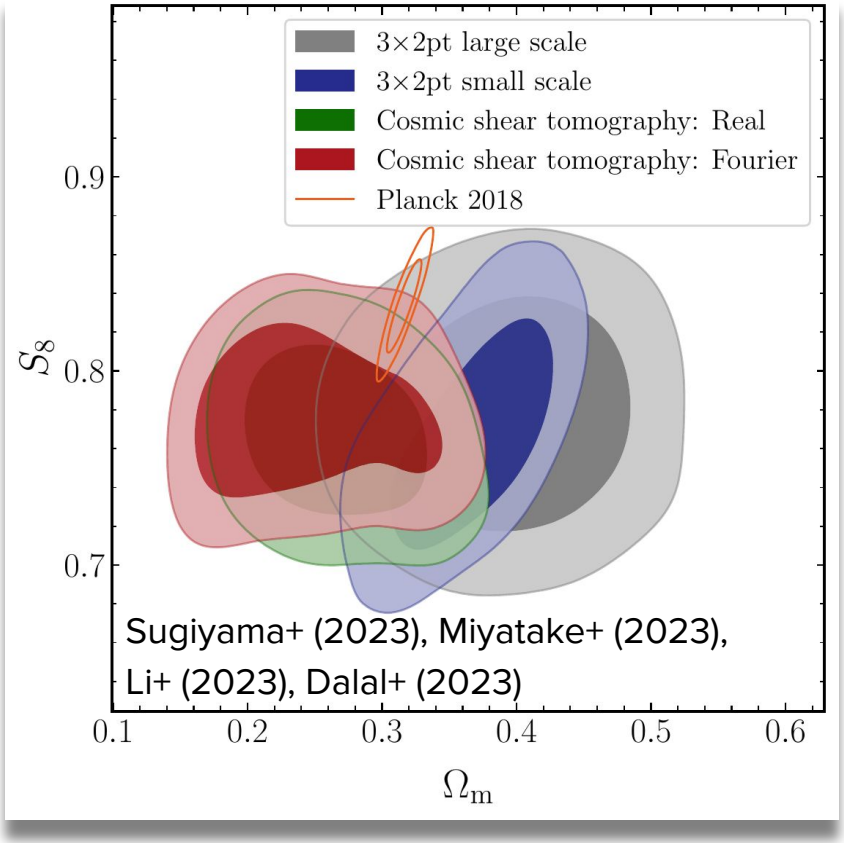
$$S_8 = 0.776^{+0.032}_{-0.033}$$

Dalal, .. SM, et al. 2023
(fourier space)



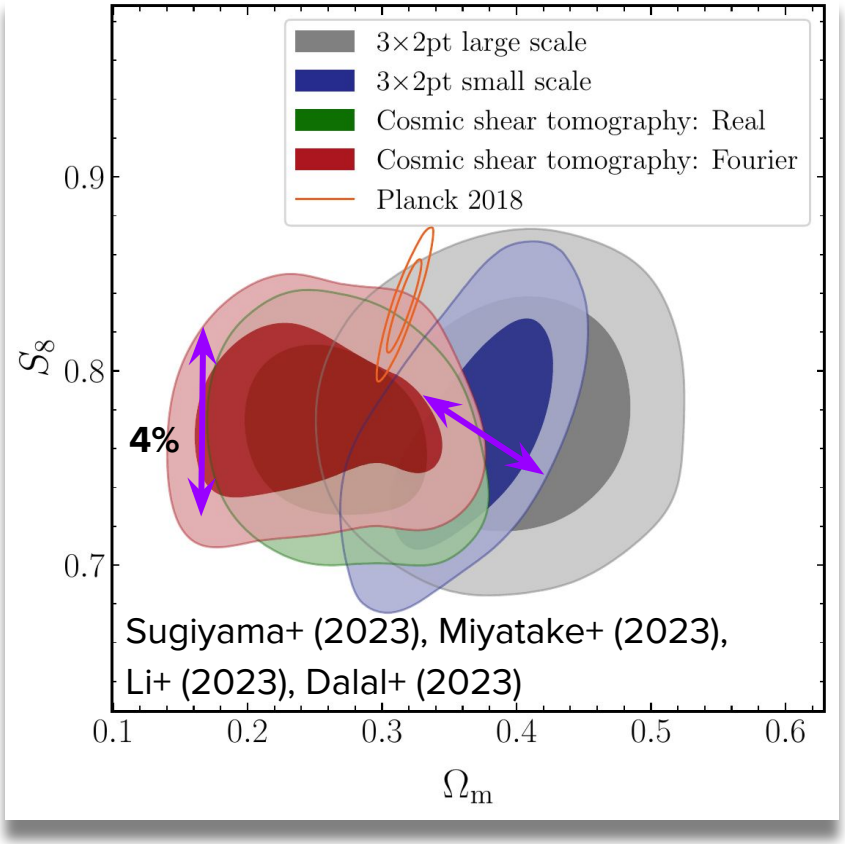


Cosmological constraints



- Consistent cosmological constraints from blind analyses
  - Cosmic shear (Real and Fourier space)
  - 3x2 pt analysis (Linear and Quasi-linear scales)
- Difference from the CMB expectation in LCDM model context based on various tension metrics range from 2-2.5 sigma
- Conservative analyses in the presence of systematic uncertainties in the redshifts of source galaxies
  - Shear-ratio test currently in progress

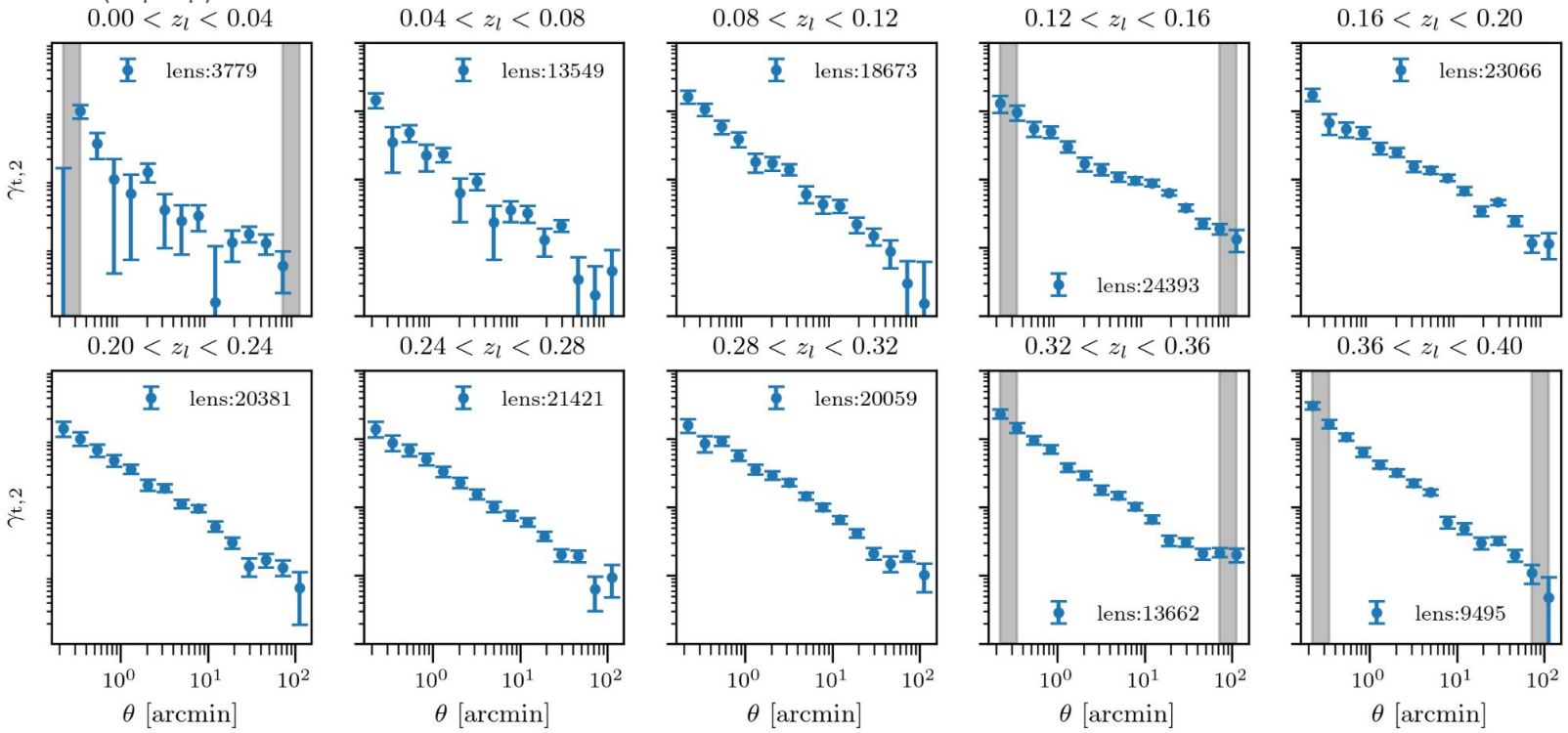
Cosmological constraints



- Consistent cosmological constraints from blind analyses
  - Cosmic shear (Real and Fourier space)
  - 3x2 pt analysis (Linear and Quasi-linear scales)
- Difference from the CMB expectation in LCDM model context based on various tension metrics range from 2-2.5 sigma
- Conservative analyses in the presence of systematic uncertainties in the redshifts of source galaxies
  - Shear-ratio test currently in progress

Shear on a set of lens galaxies: source bin 2

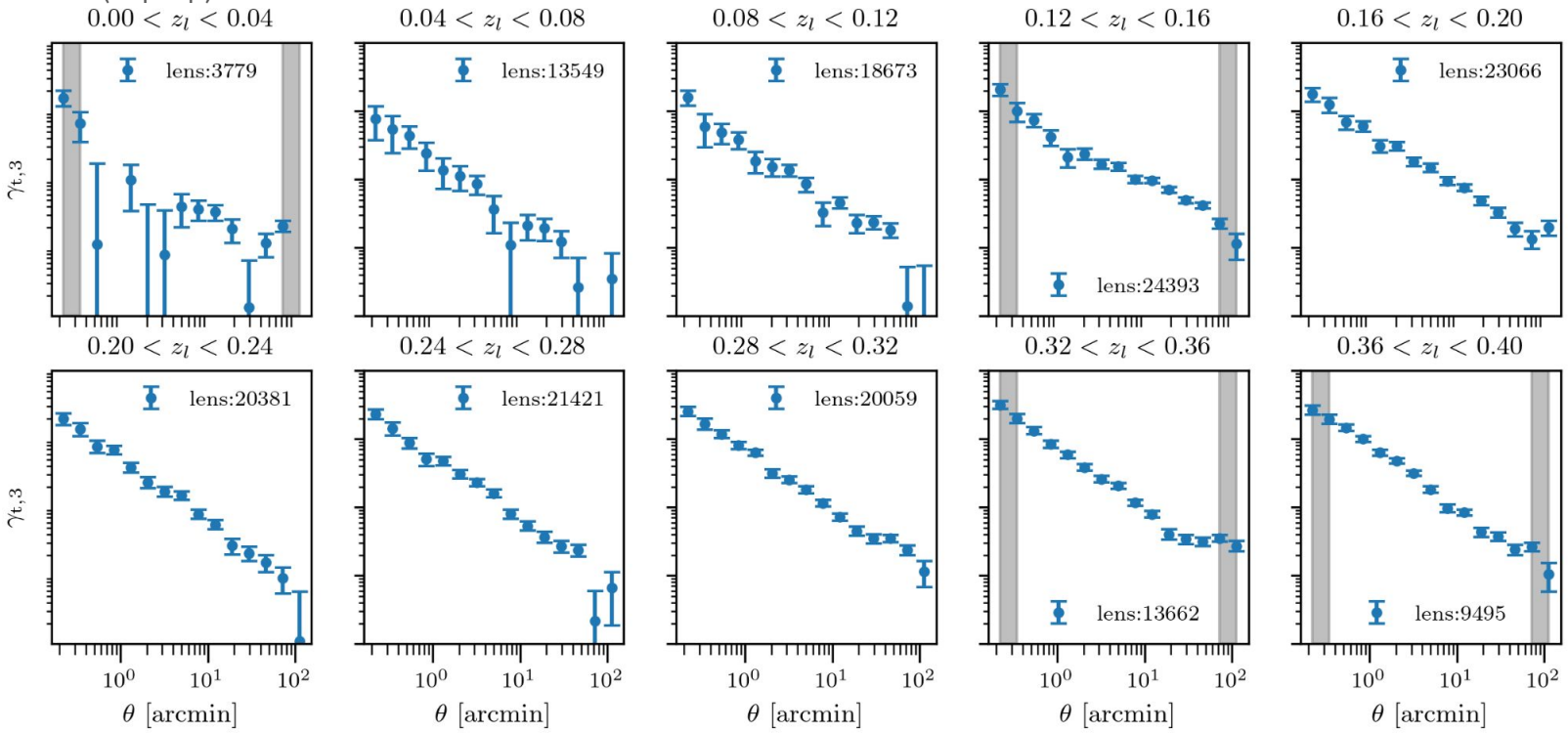
Rana, SM et al. (in prep)



Signal strength increases as we use lenses from higher redshift bins.

Shear on a set of lens galaxies: source bin 3

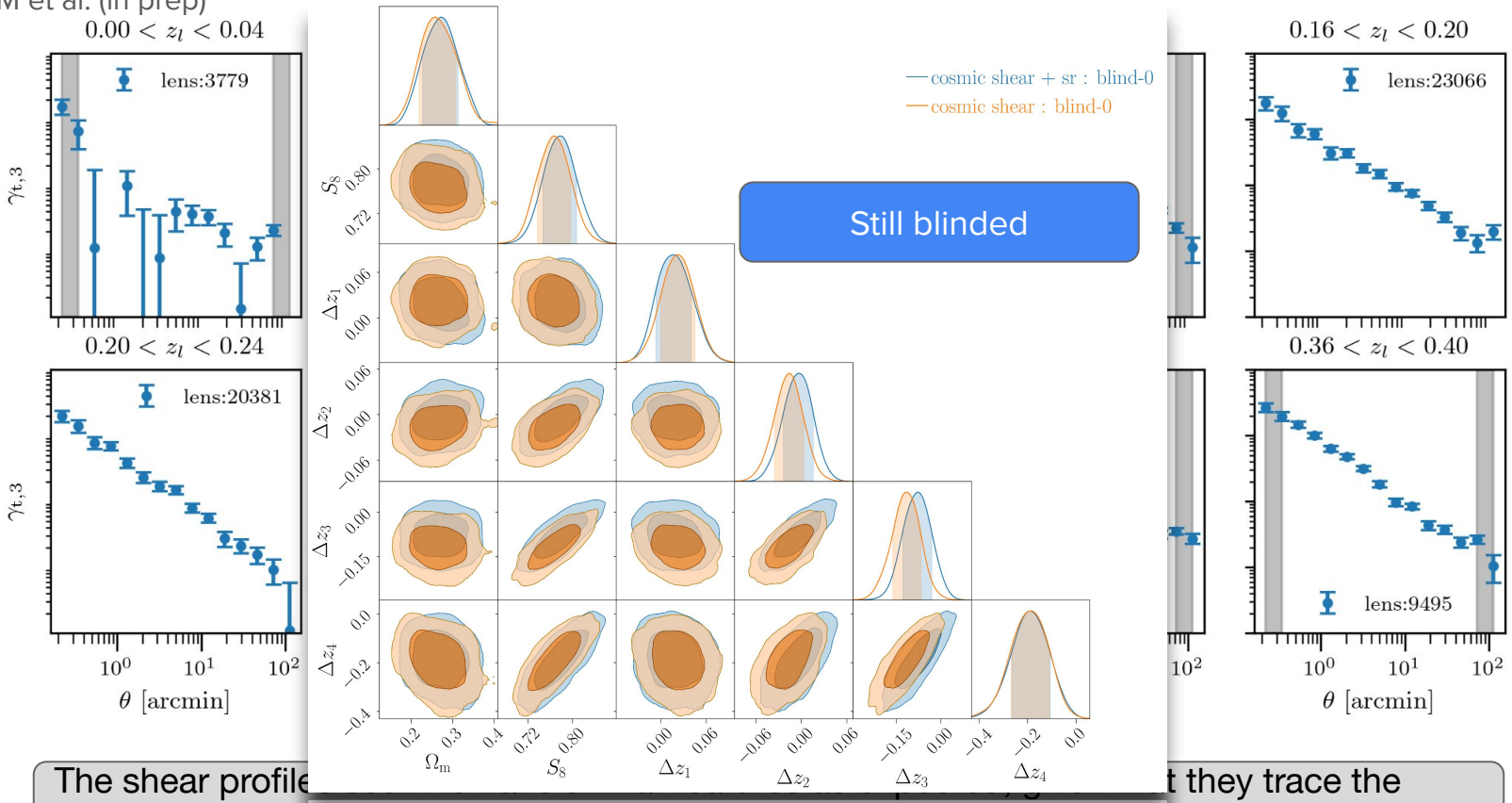
Rana, SM et al. (in prep)



The shear profiles seem to have similar features as expected, given that they trace the same lens distribution

Shear on a set of lens galaxies: source bin 3

Rana, SM et al. (in prep)



The shear profile… …t they trace the same lens distribution

Summary

- Cosmological constraints from the Subaru Hyper Suprime-Cam survey 3 year shape catalog data
  - Cosmic shear measurements and constraints
  - Joint analysis of galaxy clustering, galaxy galaxy lensing signal, and cosmic shear
- Constraints on the amplitude of density fluctuations
  - S_8: $0.78^{+0.03}_{-0.03}$ from cosmic shear alone
  - S_8: $0.76^{+0.04}_{-0.04}$ from clustering, lensing and cosmic shear combination
  - Biggest uncertainty currently due to the systematic biases in the redshift distribution of HSC galaxies
- More to come from the galaxy surveys
  - Subaru HSC final data release analysis, DES Y6 analysis

Stay tuned for more!

Thank you!

